2023 6(3):192-217

DOI 10.31462/jcemi.2023.03192217



RESEARCH ARTICLE

Gaussian Plume Modelling for an industrial facility in Karabük Province

Ali Can¹, Mohamed A. Lefghih¹

¹ Karabuk University, Faculty of Engineering, Mechanical Engineering Department, Karabük, Türkiye

Article History

Received 31 July 2023 Accepted 04 September 2023

Keywords

Industrial emissions Gaussian plume model Emission dispersion Air quality

Abstract

Industrial growth has led to an increase in pollutant and greenhouse gas emissions, further contributing to global climate change. To mitigate their environmental impact and environmental consequences, accurate estimation of pollutant dispersion and concentrations released from industrial stacks is important. This work proposes a study on the emissions of an industrial establishment in Karabük Province. The computer simulation program within Microsoft Excel that employs the Gaussian Plume (GP) model is used to predict distributions of SO₂, CO₂, CH₄, and N₂O concentrations for emissions from point sources of the industry. The results have shown that the dispersion does not depend only on atmospheric conditions but also depends on the physical conditions of the industrial facility. The plume height, effective plume height and pollutant concentrations are very important physical variables of the industrial facility. Any of them is very crucial for pollutant concentrations exposed at the ground-level. For that reason, these parameters for the industry are collected carefully. The industry is situated in Karabük province. The establishment has two stacks: one of them is very high (48 m) and the other one is (25 m) almost half of the first one. The model results have shown that the emission from the lowest stack is very high as compared to the higher one. Twodimensional modeling results are obtained from the EXCEL Program. However, the output of the model can also be shown as 3- dimensional by using the MATLAB Program. 3- dimensional results show the pollutant distribution in a better way.

1. Introduction

The impacts of air pollution on both human health and the environment are very important. The emissions from the sources are different and their effects on the environment sometimes cannot be estimated. The emitted pollutants into the atmosphere, as being the primary pollutants, give different hazardous effects after they enter physical and chemical reactions in the atmosphere [1]. Therefore, each pollutant including PM and pollutant gases have to be considered separately and evaluated in detail. Among different pollutants,

there is SO₂ which is due to the combustion of fossil fuels containing sulfur and there are greenhouse gases (GHGs) which are CO₂, CH₄ and N₂O. CO₂ emission is responsible for climate change for about 60% [2, 3].

Air pollution is primarily caused by human activities [4]. Anthropogenic air pollution has long been recognized as a severe environmental and public health issue [5]. Anthropogenic activities include burning fossil fuels and biomass in commercial and residential areas, domestic drainage, agricultural activities, vehicle

transportation, industrial activities, bunkers, etc. They all emit different pollutant gases into the atmosphere [6].

Emissions from different sources are dispersed and transported to the receptors [7]. Different effects of pollutants are seen on the receptors. However, it is very difficult to determine the total effect of pollutants on the receptors. The effect of each pollutant is different at different distances [8]. Therefore, the main goal is to decrease the emission of pollutants from different sources to decrease their effects on the environment [9]. Clinical, epidemiological and animal studies demonstrate that exposure to an emitted chemical is highly associated with chronic effects [4]. Therefore, breathing in dust and gases can be harmful to human health in many ways especially SO₂ is quite harmful because it is an acidic gas. It may also lead to severe poisoning, destroy flora and fauna, and even cause corrosion and harm to buildings and historical monuments [6, 10].

The amount of pollutants emitted into the atmosphere is limited by "emission standards" set by the government. Also, there are immission standards to achieve legal levels of ambient air purity known as "air quality standards" [11]. Ambient air quality in cities, rural areas, and even in isolated local places varies from hour to hour, day to day, and year to year [12, 13].

Air quality modeling is a powerful tool for environmental scientists, engineers, and policymakers to estimate the concentration of pollutants at any point. Different numerical models can be used to predict the effects of emissions from different sources. Dispersion modeling calculates concentrations of pollutants at various sites by using mathematical equations that describe the atmosphere, dispersion, convection, chemical and physical processes together with plume properties [14, 15]. Emission rates of pollutants, atmospheric properties, and receptor data make up the main inputs of the dispersion model [15, 16].

Some models are very useful and accurate as compared to the others. Although, the Gaussian Plume (GP) Model has some assumptions, using the GP Model provides a lot of advantages to the users,

especially for emissions from point sources [17]. With this model dispersion of pollution from point sources can be calculated easily. The main parameters of this model are emission rate from the stacks, plume height, atmospheric stability, wind speed, dispersion and convection directions and distance from the emission source [18]. The GP model gives an idea of how much pollution concentrations will be felt by the receptor at any point [17, 19]. It helps local authorities for considering the impact of emissions on local territory [20, 21, 22]. Urban air pollution is a major environmental problem in Türkiye [23]. Türkiye had an Air Quality Regulation in effect since 1986 [24]. Due to growing urbanization, air quality in Türkiye is limited to a few contaminants. However, they are regionally and temporally indicative of the actual conditions due to the setup of monitoring stations [25].

The ambient concentrations and deposition rates of many chemicals in the atmosphere can also be calculated by using air quality models [26]. A numerical approach or methodology for calculating air pollutant concentrations over time and space is known as "air quality simulation model system (AQSM)". The effectiveness of simulations can be increased by considering many parameters under the technique of Geographical Information System (GIS) [27].

In this study, the main goal is to determine the effects of air pollution caused by an industrial facility in the Karabük Province. The studies are concentrated on the Gaussian Plume model. To run this model. meteorological and physical parameters, and the emission discharge rates are required. The detailed descriptions are given in the Methodology section. The final results are evaluated according to the outputs of the GP Model. The pollution created especially by SO₂, CO₂, CH₄ and N₂O is described and their possible effects are considered on a scientific basis. The results of this study can be used for city management strategies and air quality problems in the Karabük Province.

2. Methodology

The focus will be on modeling and creating simulation software by using Microsoft Excel. This program will help us to simulate and understand how pollutants spread from a point source in the environment. Air pollution in the industry is caused by various activities that release gases into the atmosphere. Among these gases, SO₂, CO₂, CH₄, and N₂O are the most important ones that pollute the atmosphere. Therefore, this study aims to develop a simulation tool that accurately estimates concentration levels of these pollutants using point source models. The processes are mainly divided into three categories. These are data input, data

processing and data analysis [28] as depicted in Fig. 1

Data input: Data is collected to feed into the model software. The data must include the atmospheric parameters, the source emissions, and physical details of the source. Tier 1 methodology of the IPCC [29] has been applied. By the way, the necessary permission from the industrial facility in the Karabuk area could not be taken for sharing the name of the facility. The privacy legacy prohibits the usage of daily emission data. The management board was only permitted to share the daily fuel consumption data by hiding the name of the industrial establishment. Therefore, daily fuel consumption data was used in this study.

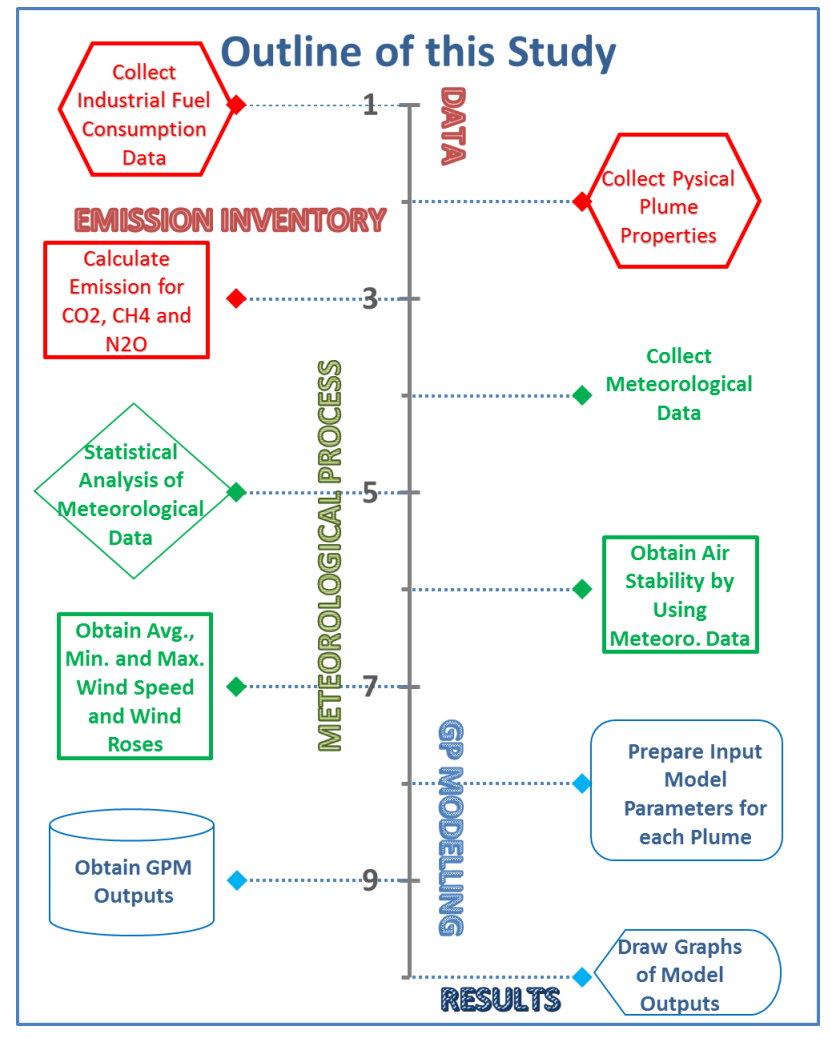


Fig. 1. Outline of this study

Data processing: Some gathered data from the establishment such as physical stack height and emission rates were used directly in the model. The others such as wind speed, atmospheric cloudiness, sunset hours, solar radiation and wind directions obtained from Turkish were the State Meteorological Service (TSMS). They were used for the determination of atmospheric stability classes. Then, the processing of the emission data for the selected zone in the model was completed to desired ground-level pollution obtain the concentrations.

Data analysis: The final step involves analyzing the ground-level pollutant concentrations and mortality percentages for the selected zone. Results were evaluated to determine any potential consequence of the obtained ground-level pollutant concentrations on the environment and human

health. This section is the most important, and the results must be evaluated in the direction of wind speed.

2.1. Emission Calculation

The emission estimates were done by using the industrial fuel consumption data. However, the details of the industrial data were not given due to a signed secrecy agreement between Karabuk University and the company. For the reason of privacy protection, industrial data was disclosed only for daily minimum, maximum and average fuel consumption.

The company uses two types of fuel. The main fuel is lignite, and the auxiliary fuel is fuel oil. The amount of fuel consumed by the company is given only on the daily minimum, maximum and average basis in Table 1.

Table 1. Daily minimum, maximum and average values of fuel consumption

| Unit (| (kg) | May- 22 | Jun- 22 | Jul- 22 | Aug- 22 | Sep- 22 | Oct- 22 | Nov- 22 | Dec- 22 | Jan- 23 | Feb- 23 | Mar- 23 | Apr- 23 |
|---------|-----------------|------------|------------|------------|------------|------------|------------|------------|------------|------------|------------|------------|------------|
| | | | | | | Li | gnite | | | | | | |
| | Min | 51 | 45 | 67 | 80 | 75 | 65 | 60 | 35 | 35 | 47 | 60 | 78 |
| | Max | 98 | 120 | 160 | 170 | 165 | 120 | 120 | 98 | 94 | 110 | 123 | 134 |
| | Avg | 75.7 | 109.5 | 136.6 | 150.9 | 136.2 | 116.1 | 109.3 | 71.0 | 69.4 | 85.7 | 90.3 | 108.2 |
| le 1 | Monthly Tot. | 2348 | 3286 | 4235 | 4678 | 4086 | 3600 | 3280 | 2200 | 2150 | 2400 | 2800 | 3245 |
| Plume 1 | | | | | | Fu | el-Oil | | | | | | |
| щ | Min | 5 | 5 | 7 | 8 | 8 | 7 | 6 | 4 | 4 | 5 | 6 | 8 |
| | Max | 10 | 13 | 17 | 18 | 17 | 13 | 13 | 10 | 10 | 12 | 13 | 14 |
| | Average | 8.0 | 11.7 | 12.9 | 13.9 | 13.3 | 9.7 | 9.3 | 7.7 | 6.5 | 8.0 | 8.1 | 10.3 |
| | Monthly Tot. | 248 | 350 | 400 | 430 | 400 | 300 | 280 | 240 | 200 | 225 | 250 | 310 |
| | | | | | | Li | gnite | | | | | | |
| | Min | 15 | 15 | 15 | 18 | 23 | 21 | 26 | 22 | 18 | 16 | 17 | 22 |
| | Max | 50 | 56 | 57 | 67 | 70 | 80 | 75 | 65 | 60 | 63 | 68 | 43 |
| | Average | 35.5 | 36.7 | 35.5 | 43.4 | 52.0 | 54.8 | 56.7 | 43.5 | 41.9 | 43.6 | 41.9 | 35.5 |
| Plume 2 | Monthly Tot. | 1100 | 1100 | 1100 | 1345 | 1560 | 1700 | 1700 | 1350 | 1300 | 1220 | 1300 | 1065 |
| Plu | | | | | | Fu | el-Oil | | | | | | |
| | Min | 2 | 2 | 2 | 2 | 3 | 2 | 3 | 3 | 2 | 2 | 2 | 3 |
| | Max | 6 | 6 | 6 | 8 | 8 | 9 | 9 | 7 | 7 | 7 | 8 | 5 |
| | Average | 4.0 | 4.2 | 4.0 | 4.8 | 5.7 | 5.8 | 6.2 | 4.7 | 4.1 | 4.5 | 4.1 | 3.7 |
| | Monthly Tot. | 125 | 125 | 125 | 150 | 170 | 180 | 185 | 145 | 128 | 125 | 128 | 110 |

These fuels are combusted, and the emissions are given to the atmosphere by two stacks. One of the stacks is 48 m tall and the other is 25 m tall. The gas flow rates, velocities and exit densities from these two stacks are given in Table 2.

The IPCC method was used as a default. For obtaining CO₂ emissions. Eq. (1) is used to calculate the greenhouse gas emissions by using the Emission Factors (EF) given in the IPCC:

$$ER_{GHG, fuel} = FC_{fuel} * EF_{GHG, fuel} * CF_{fuel cal,}$$
 units, carbon content (1)

where,

 $ER_{GHG, fuel}$: the strength of the emission source (equal to Q),

 FC_{fuel} : fuel consumption rate,

 EF_{GHG} , fuel: IPCC default emission factors,

*CF*_{fuel cal, units, carbon content}: conversion factors for fuel calories, units and carbon content.

The IPCC SO₂ Emission Factors, however, have to be calculated depending on the sulfur content of the fuel, retention of sulfur in ash, net calorific value of fuel and efficiency of abatement technology as given in Eq. (2):

$$EF_{SO2} = 2 * \frac{s}{100} * \frac{1}{NCV} * 10^6 * \frac{100 - r}{100}$$

$$* \frac{100 - n}{100}$$
(2)

where,

EF_{SO2}: emission Factor (kg/TJ),

 SO_2/S : default value is 2 (kg/kg),

s: Sulphur content in fuel (%),

r : retention of Sulphur in ash (%), *NCV* : net calorific value (TJ/kt),

10⁶: unit conversion,

n: efficiency of abatement technology and/or reduction efficiency (%).

The emission calculations are estimated by using default emission factors (EFs), which means the EFs of IPCC method are internationally consistent and they must be preserved for comparability of any inventory using this method. The default carbon and sulfur contents, net calorific values, unit conversion, efficiency and/or retention in ash are determined due to the countries' reports by IPCC experts. Although these parameters are changing greatly in countries' inventories, global default EFs, especially for IPCC-T1 calculations, are advised to be used for countries in their emission inventories. The respective EFs of Lignite and fuel oil are 27.6 tC/TJ and 21.1 tC/TJ, respectively. The details are given in Appendix B. The sulfur content(s) in the lignite and fuel oil are taken as 1.5% and 3%, respectively. The net calorific value (NCV) in the lignite and fuel oil are taken as 40.55 TJ/kt and 11.14 TJ/kt, respectively, in the calculations.

2.2. Gaussian Plume Model (GPM)

The concentration of a pollutant is described by the GP model as a vertical and horizontal function of a Gaussian bell shape curve. The plume of the model allows to estimate the concentration of pollutants at any location. Gaussian model strongly depends on atmospheric stability and meteorological conditions [30, 31]. A schematic representation of the GPM is given in Figure 2.

The three-dimensional diffusion equation for atmospheric dispersion is given by Eq. (3):

$$\frac{\partial \chi}{\partial t} = \frac{\partial}{\partial x} \left[K_x \left(\frac{\partial \chi}{\partial x} \right) \right] + \frac{\partial}{\partial y} \left[K_y \left(\frac{\partial \chi}{\partial y} \right) \right] + \frac{\partial}{\partial z} \left[K_z \left(\frac{\partial \chi}{\partial z} \right) \right]$$
(3)

where,

Table 2. Stacks Properties

| Table 21 Stacks 1 Toper des | | |
|---|-----------|-----------|
| Stracks Properties | Stack 1 | Stack 2 |
| Stack Height (m) | 48 | 25 |
| Gas Exit Temp (°C) | 550-600 | 450-580 |
| Gas Exit Densities (kg/m3) | 1.1-1.185 | 1.1-1.185 |
| Avg. Gas Exit Velocity (m/s)* | 0.4 | 0.2 |
| Avg. Gas Exit Flowrate (m ³ /s)* | 1.81 | 0.40 |

^{*} Measurements are made twice a month

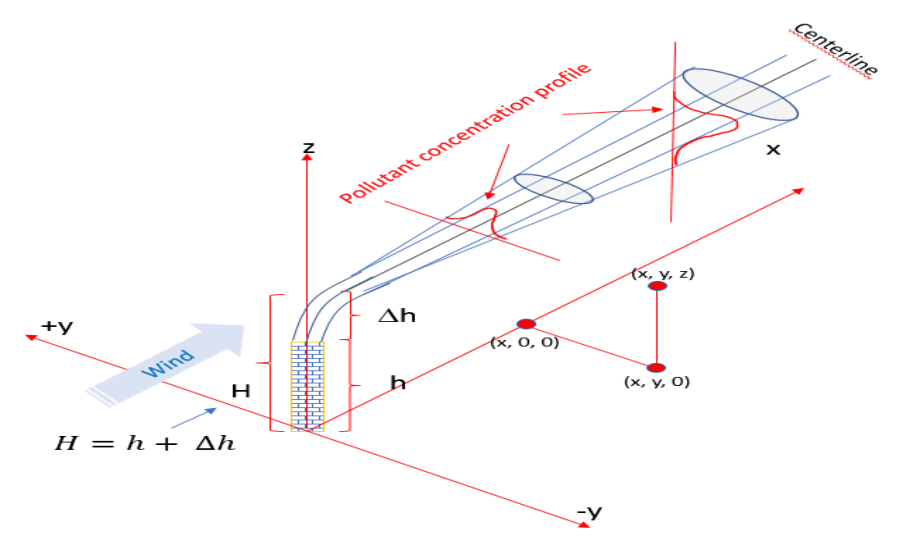


Fig. 2. Gaussian Plume Model

x, y and z: the downwind, crosswind and vertical directions, respectively.

 K_x , K_y , K_z : Diffusivities in x, y and z directions.

The general solution of this second-order partial differential equation at steady state is given by Eq. (4):

$$C = K_{bc} x^{-1} exp \left\{ -\left[\left(\frac{y^2}{D_y} \right) + \left(\frac{z^2}{D_z} \right) \right] \frac{u}{4x} \right\}$$
 (4)

where,

 $C_{(x, y, z)}$ or C: mean concentration of the diffusing substance at a point (x, y, z) [kg/m³],

 D_y , D_z : mass diffusivities in the direction of y and z axes, respectively [m²/s],

u: mean wind velocity along the x-axis [m/s],

 K_{bc} : constant determined due to a boundary condition.

Here K_{bc} is an arbitrary constant. If it is substituted in Eq. (4),

$$Q = \iint_{-\infty}^{+\infty} U K_{bc} x^{-1} \exp\{-\left[\left(\frac{y^{2}}{K_{y}}\right) + \left(\frac{z^{2}}{K_{z}}\right)\right] \frac{u}{4x} \} dy dz$$
 (5)

Eq. (5) is obtained. In this equation, K is defined as:

$$K = \frac{Q}{4\pi (D_{\nu}D_{z})^{1/2}} \tag{6}$$

Then, Eq. (4) for concentration C becomes,

$$C(x,y,z) = \frac{Q}{4\pi x (D_y D_z)^{\frac{1}{2}}}$$

$$exp \ exp \left[-\left(\frac{y^2}{D_y}\right) + \frac{z^2}{D_z} \right] \frac{U}{4x}$$

$$(7)$$

here Q is the strength of the emission source, mass emitted per unit time. Eq. (7) gives the concentration at any x, y and z.

Dispersion coefficients in the y and z directions are a measure of the change in the concentration of the pollutant in the y and z directions. In statistics, these changes are known to be standard deviations which are expressed as σ_y in the horizontal direction and σ_z in the vertical direction. Σ_y and σ_z are expressed as follows in Eq. (8):

$$\sigma_y = \sqrt{2D_y \frac{x}{u}} \text{ and } \sigma_z = \sqrt{2D_z \frac{x}{u}}$$
 (8)

From these equations D_y and D_z are expressed as follows:

$$Dy = \frac{\sigma_y^2}{2x} u Dz = \frac{\sigma_z^2}{2x} u$$
 (9)

By placing Eq. (9) into Eq. (7), the final Eq. (10) is obtained which is the final equation to calculate the pollutant concentration at any x, y and z within the plume. This equation is known as a Gaussian Plume Model (GPM).

$$C(x, y, z) = \frac{Q}{2\pi u \sigma_y \sigma_z}$$

$$* \left\{ exp \ exp \left(\frac{-(z - H)^2}{2\sigma_z^2} \right) + exp \ exp \left(\frac{-(z + H)^2}{2\sigma_z^2} \right) \right\}$$

$$* \ exp \left(\frac{-(y)^2}{2\sigma_y^2} \right)$$

Atmospheric stability is divided into six stability classes by Pasquill (Table 3). Class A denotes the most stable condition, and class F denotes the most unstable and turbulent condition [32].

The GP model is derived with some assumptions. The first assumption is related to the emission rate which is assumed to be constant, which means a steady state condition prevails. The emissions are assumed to be chemically inert materials and expected as non-reactive. The exponential decay factor is also related to the distances. As the distance from the source increases, concentration decreases exponentially. The last and most important assumption is that the wind speed remains constant with height. This is never the actual case. These assumptions increase the uncertainty level of the model and decrease the some sensitivity of parameters. Gaussian distribution is simply a function of distance on x direction from the source and it describes lateral and longitudinal changes in the concentrations. Decreasing the uncertainty level can be achieved by using the average and statistically evaluated meteorological data. To avoid the adverse effect of these assumptions, many statistical analyses are

made to synchronize the emission data, thus minimum, maximum and average parameters are obtained. To increase the reliability of the model, every parameter is evaluated scientifically. The plume ascent is even calculated by using Holland's Equation as seen in Eq. (11) [33]:

$$\Delta h = \frac{v_s d_s}{u} \left[1.5 + (2.68 \times 10^{-3}) P_a \left[\frac{T_s - T_a}{T_c} \right] d_s \right]$$
 (11)

where,

 Δh : rise of the plume above the stack (m)

u: wind speed at stack height $\left(\frac{m}{s}\right)$

 v_s : stack gas velocity $\left(\frac{m}{s}\right)$

 d_s : inside stack diameter (m)

 P_a : atmospheric pressure (mb)

 T_s : stack gas temperature (K)

 T_a : atmospheric temperature (K)

2.3. The GPM Programme

The Gaussian Plume Model (GPM) provides mathematical concentration interfaces by entering essential information into the program including physical and meteorological variables related to atmospheric stability, terrain, plume characteristics and metrological conditions. The model Program (Figure 3) consists of three levels, each of which uses necessary parameters for accurate dispersion calculations [34]. For properties of Stacks see Table 2. The input examples for Stack 1 and Stack 2 are given in Appendix C.

Table 3. Pasquill atmospheric stability classes [32]

| W' G 1 - | Dayti | me Solar Insolation (V | V/m^2) | Night | | | |
|----------------|--------------|------------------------|--------------|-----------------|-------------|--|--|
| Wins Speed m/s | Strong > 600 | Moderate 300-600 | Slight < 300 | Low cloud ≥ 4/8 | Cloud ≤ 3/8 | | |
| < 2 | A | A-B | В | - | - | | |
| 2-3 | A-B | В | C | E | F | | |
| 3-5 | В | В-С | C | D | E | | |
| 5-6 | C | C-D | D | D | D | | |
| > 6 | C | D | D | D | D | | |



Fig. 3. EXCELL-based GPM Programme

Atmospheric stability: Users can enter particular codes that correlate to the stability class according to the wind speed, atmospheric cloudiness, weather temperatures and daytime to represent atmospheric conditions. By entering the necessary parameters users can correctly define the atmospheric condition.

Plume and industrial characteristics: Emission rate, physical stack height, and effective stack height are the most important parameters. These parameters directly affect the resulting pollutant concentration and contribute to the initial conditions of the dispersion model.

Wind data: Users can enter the metrological information related to wind speed and direction. Averaged or hourly wind speed and wind directions for the study period have to be entered into the program for the dispersion and transportation directions, which allows for a realistic depiction of the plume flow.

Maximum distance: Users can input the maximum X and Y distances, which describe the spatial extent for dispersion calculations.

Results

The results have shown that the industrial facility is affecting the atmosphere in different ways. Especially the effect of SO₂ is very important. Each way including the SO₂ and GHGs emissions, the

meteorological data processing and their analyses have been considered separately in this study.

3.1. The SO₂ and GHG emissions

This section contains two main steps. The first one is collecting the fuel consumption data for the industry. The second one is the calculation of the GHG emissions.

Fuel Consumption Data: Fuel consumption data is crucial to calculate energy consumption and emissions. This analysis provides valuable insights into the fuel consumption patterns for the specified period. Data is available from May 2022 to April 2023. The industry uses lignite as the main fuel. The auxiliary fuel is fuel oil in smaller quantities. The fuel consumption data are analyzed to determine the minimum, maximum, and average daily fuel quantities in each month and the total monthly usage of fuels for the industrial facility is found. This analysis will reveal the energy consumption patterns of the industry, as well as any inefficiencies and trends in fuel usage over the study period. The daily minimum, maximum and average fuel oil and lignite consumptions are given for the company in Table 1. The monthly consumption of fuel oil and lignite is calculated according to the average values (Table 1).

Emission Inventory: One of the most important tasks for the modeling process is the emission calculation. The emission value is the main

parameter for GPM. Therefore, the collected fuel oil and lignite consumption values of the industry used for calculating the ground-level concentrations of SO₂, CO₂, CH₄, and N₂O. The environmental impact of the industry can be assessed identifying emissions and concentration patterns. Concentrations are presented by using graphs. It can be observed from the figures that the emissions vary throughout the entire study period, and they cause different ground-level concentrations owing to the change of other parameters. The annual equivalent CO₂ emission from the industry is around 0.243 million tons. This quantity expresses the total CO2 equivalent of the greenhouse gas emissions. Control strategies have to be improved to decrease the greenhouse gas emissions.

The minimum, maximum and average daily CO₂ emission are given in Figure 4. The average daily CO₂ emission in some days reaches 0.57 Gigagram in Stack 1. This quantity is high. However, the effect on the ground-level concentration is not high as compared to Stack 2. The main reason is the height of the stacks. The emissions are emitted to the atmosphere at a level

of 48 m in Stack 1. However, in Stack 2 this level is 25 m. This means the ground-level concentration for the second plume can be very high depending on the atmospheric conditions.

The concentrations of CH_4 and N_2O are also calculated for each plume. The concentrations are very low as compared to CO_2 concentration. The CH_4 emission is considered an incomplete combustion product of fossil fuels. The atmospheric nitrogen is also very effective for the emission of N_2O . The ratios of both gases are very low compared to the CO_2 . However, CO_2 equivalent values for CH_4 and N_2O are 21 and 310, respectively.

This means that one mole of CH_4 and one mole of N_2O emission create 21 and 310 times more greenhouse effect, respectively, than one mole of CO_2 emission [35].

Emission calculations offer valuable insights into the minimum, maximum, and average quantities of generated GHG emissions (Figure 5).

Emission Inventory for SO_2 : The annual SO_2 emission value from the industry is around 14.20 million tons.

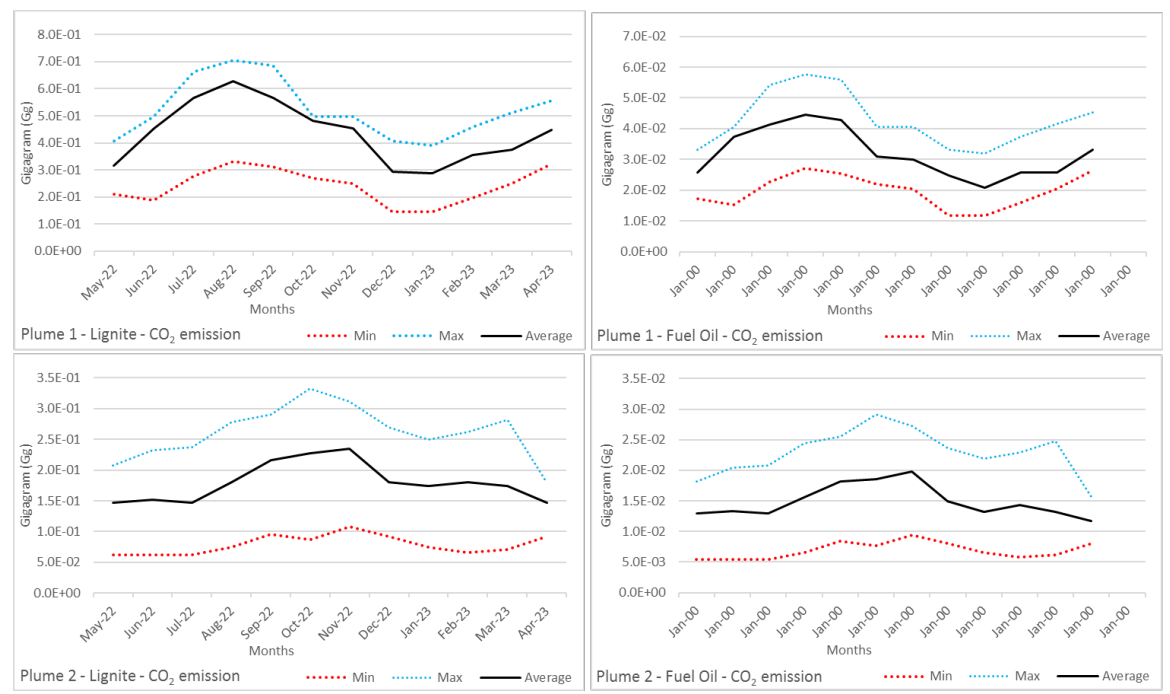


Fig. 4. Daily minimum, maximum, and average CO₂ emission from stacks

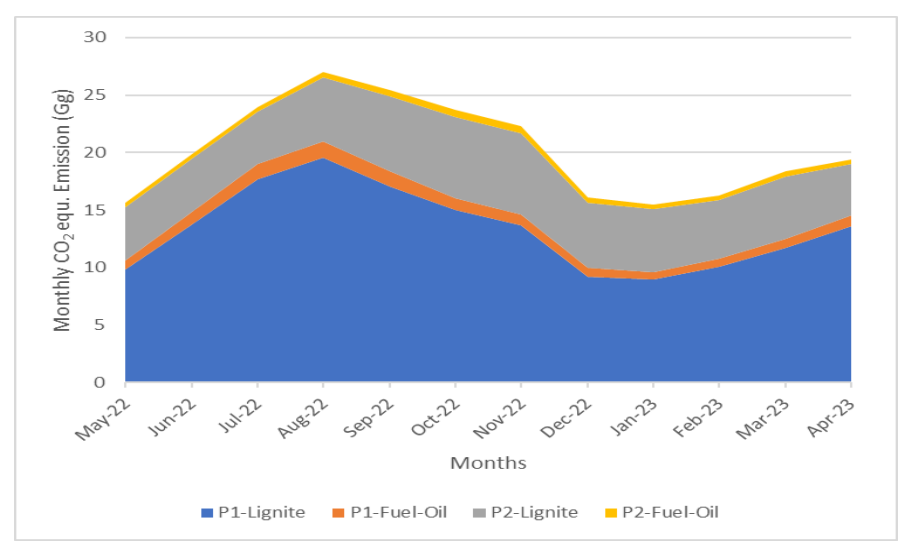


Fig. 5. Annual CO₂ equivalent GHG emission from the industrial establishment

This quantity for an industry is too high. The control strategies have to be improved for general public health, even if the SO₂ emissions in both stacks are reduced by abatement technology. The average reduction efficiency is around 60%.

The minimum, maximum and average daily SO₂ emissions are given in Figure 6. The average daily SO₂ emission in some days reaches 0.036 Gigagram in Stack 1. This quantity of SO₂ for the industry is

very high and it has to be decreased by improving the efficiency of the abatement technology.

Emission calculations offer valuable insights into the minimum, maximum, and average quantities of SO_2 emissions.

The trendlines of SO₂ and GHGs are very familiar due to the consumed fuel quantity (Figure 7).

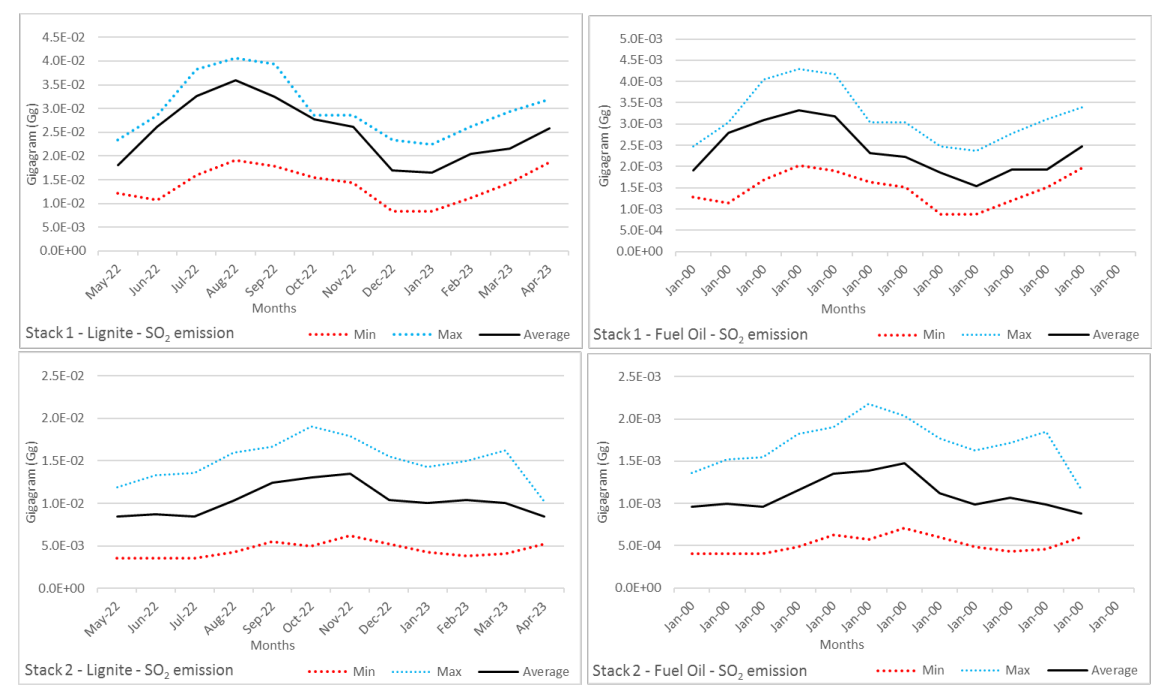


Fig. 6. Daily minimum, maximum, and average SO₂ emission from stacks

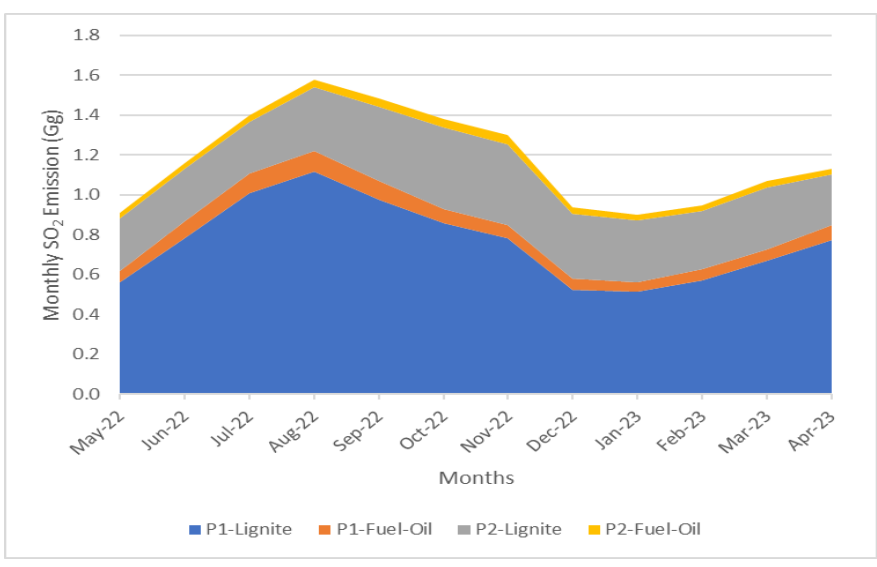


Fig. 7. Annual SO₂ emission from the industrial establishment

The simple method (Tier 1 method of IPCC) is preferred for the emissions calculations. This standard methodology requires fuel consumption quantity and emission factors (EF). Therefore, the different EFs give different quantities, but it does not change the trendline. The same trendline figure is also obtained for the annual SO₂ emission. The SO₂ emissions are changing between 0.912 Gigagram and 1.576 Gigagram in a year.

3.2. The Meteorological Data Processing

The metrological data used in this study was obtained from the TSMS.

This comprehensive dataset encompasses various key parameters, including wind speed, wind direction, cloudiness, and sunshine.

The dataset used for the wind analysis in this study covers the period from May 2022 to April 2023. Monthly average wind speed is calculated by using hourly data. The average data for minimum, maximum, and average wind speeds are also calculated. The calculated monthly average wind speeds are given in Table 4.

When the data are observed, it is seen that the range of data varies considerably. The minimum wind speed changes between 0.0 m/s to 1.8 m/s, and the maximum wind speed changes between 1.1 m/s to 8.2 m/s. For the average wind speed, the range is determined between 0.6 m/s and 2.3 m/s.

Cloudiness data is also necessary to determine the stability classes of the atmosphere. Minimum and maximum values represent the coverage of cloudiness. The mean cloudiness over the entire month is used to determine the atmospheric cloudiness condition. Graphical representations in the form of line charts are generated to analyze and interpret the observed trends in cloudiness throughout the study. The dot in the middle of the figures represents the average cloudiness value of the related month (Figure 8).

The dataset incorporates information on the average hourly sunshine intensity and the sum of sunshine intensity per month. These data were analyzed to generate a comprehensive pattern in sunshine duration and intensity.

The stability classes were determined for 12 months by analyzing data including wind speed, cloudiness, sunshine duration, and sunshine intensity.

These derived stability classes are used in the model. The final stability classes of the atmosphere are shown in Table 5.

3.3. Concentration Maps

These maps are obtained in two forms: *Condensed form* and *3-D concentration form*.

| T-1-1- 4 M | - £i J | and a selection of the | and the second s | Latina autoria |
|--------------------------|-----------|------------------------|--|----------------|
| Table 4. Monthly average | e or wina | speeas with | respect to wind | i directions |

| Months | N | N N E | N E | E N E | Е | E S E | S E | S S E | S | S S W | S W | W S W | W | W N W | N W | N N W |
|--------|-----|-------------|--------|-------------|-----|-------------|--------|-------------|-----|-------------|--------|-------------|-----|-------------|--------|-------------|
| 1 | 1.0 | 1.2 | 1.1 | 1.2 | 1.1 | 0.9 | 1.0 | 0.9 | 0.9 | 0.9 | 0.9 | 0.8 | 0.7 | 0.6 | 0.8 | 0.8 |
| 2 | 1.2 | 1.1 | 1.2 | 1.5 | 1.1 | 1.1 | 1.2 | 1.3 | 1.2 | 1.5 | 1.4 | 1.1 | 1.3 | 0.7 | 1.0 | 0.9 |
| 3 | 1.1 | 1.1 | 1.2 | 1.3 | 1.0 | 1.1 | 1.1 | 1.1 | 1.2 | 1.3 | 1.2 | 1.0 | 0.8 | 0.9 | 0.9 | 1.2 |
| 4 | 1.2 | 1.1 | 1.1 | 1.1 | 1.0 | 1.2 | 1.4 | 1.2 | 1.4 | 1.3 | 1.6 | 1.1 | 0.9 | 1.1 | 1.2 | 1.4 |
| 5 | 1.7 | 1.2 | 1.3 | 2.2 | 1.4 | 1.6 | 1.3 | 2.1 | 1.4 | 1.6 | 1.6 | 1.5 | 1.5 | 1.7 | 1.6 | 1.9 |
| 6 | 1.2 | 1.4 | 1.3 | 2.2 | 1.5 | 1.4 | 1.4 | 1.9 | 1.6 | 1.7 | 1.5 | 1.6 | 1.7 | 1.6 | 1.2 | 1.2 |
| 7 | 1.4 | 1.2 | 1.3 | 2.3 | 1.7 | 2.0 | 2.3 | 2.3 | 2.3 | 1.6 | 1.5 | 1.6 | 1.6 | 1.9 | 1.6 | 1.3 |
| 8 | 1.4 | 1.4 | 1.4 | 2.2 | 1.6 | 1.3 | 1.4 | 1.5 | 1.5 | 1.7 | 1.6 | 1.7 | 1.8 | 1.5 | 1.2 | 1.5 |
| 9 | 1.1 | 1.4 | 1.7 | 1.5 | 1.5 | 1.4 | 1.6 | 1.5 | 1.6 | 1.5 | 1.6 | 1.9 | 2.2 | 1.2 | 0.9 | 1.5 |
| 10 | 1.2 | 1.3 | 1.5 | 1.6 | 2.0 | 1.5 | 1.4 | 1.4 | 1.3 | 1.2 | 1.2 | 0.9 | 1.2 | 0.7 | 0.8 | 1.0 |
| 11 | 1.1 | 1.1 | 1.1 | 1.7 | 1.2 | 1.4 | 1.5 | 1.4 | 1.2 | 1.1 | 0.8 | 0.9 | 0.8 | 0.7 | 0.7 | 1.1 |
| 12 | 0.9 | 1.2 | 1.4 | 1.3 | 1.2 | 1.1 | 1.1 | 1.0 | 1.1 | 1.0 | 0.8 | 0.7 | 0.7 | 0.6 | 0.6 | 0.7 |

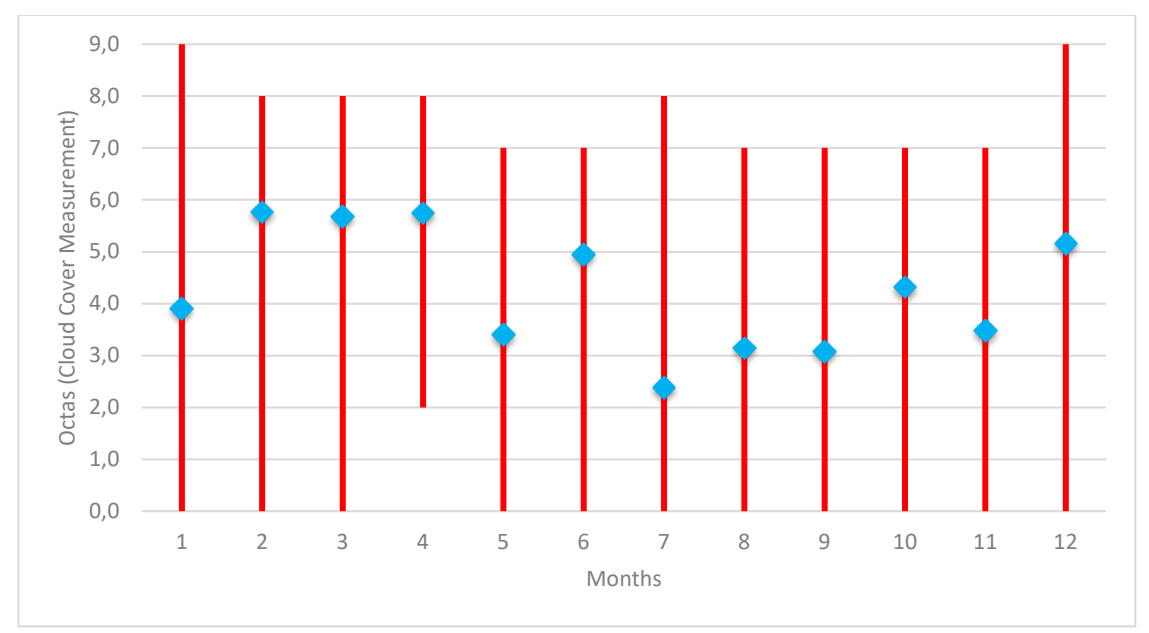


Fig. 8. Variation of monthly cloudiness

Table 5. The stability classes of the atmosphere for the study period in Karabük province

| Months | May- 22 | | | | | | Nov- 22 | | | Feb- 23 | March -23 | |
|---------|------------|---|---|---|---|-----|------------|---|-----|------------|--------------|-----|
| Min | A | A | A | A | A | A | A | В | A | A-B | A-B | A-B |
| Max | В | В | В | В | В | A-B | A-B | C | A-B | В-С | В-С | В-С |
| Average | A | A | A | A | A | A | A | В | A | A-B | A-B | A-B |

Condensed Pollution Maps: To evaluate the effectiveness of the model, results from two distinct plumes were analyzed separately. The results consisted of concentration estimations for SO₂, CO₂, N₂O, and CH₄ for 12 months, from May 2022 to April 2023. The daily minimum, maximum and average GHG concentrations are used separately to obtain concentration maps. The map output for each gas can be obtained in one run of the GPM Program. Therefore, to obtain ground-level concentrations of GHGs, the GPM Program has been run many times and each time different parameters are used.

The condensed pollution points for the average daily CO2 emissions are shown in Figure 9a. In these figures, it is very easy to see how the parameters are effective in the ground-level concentrations. When the wind speed and atmospheric stability classes are lower, the CO2 ground level concentrations are much higher as seen in December 2022. The dominant direction of pollutant dispersion changes even during the day. The statistical evaluation of the mean value for the wind direction is selected as the main direction for each month.

The comparison of concentration maps as shown in Figure 9b shows that the ground-level SO₂ concentration throughout the entire year is very effective in the province. The pollutant is dispersed densely and continuously. It is important to remember that SO2 is an acidic gas and high ground level concentrations create a health problem for the public. The ground level concentrations change throughout the entire day. Depending on the concentration level, the dispersion seems completely different compared to CO₂ as concentrations.

The comparison of concentration maps is also given in Figure 10. As can be seen in Fig. 10, the dispersion concentrations vary considerably.

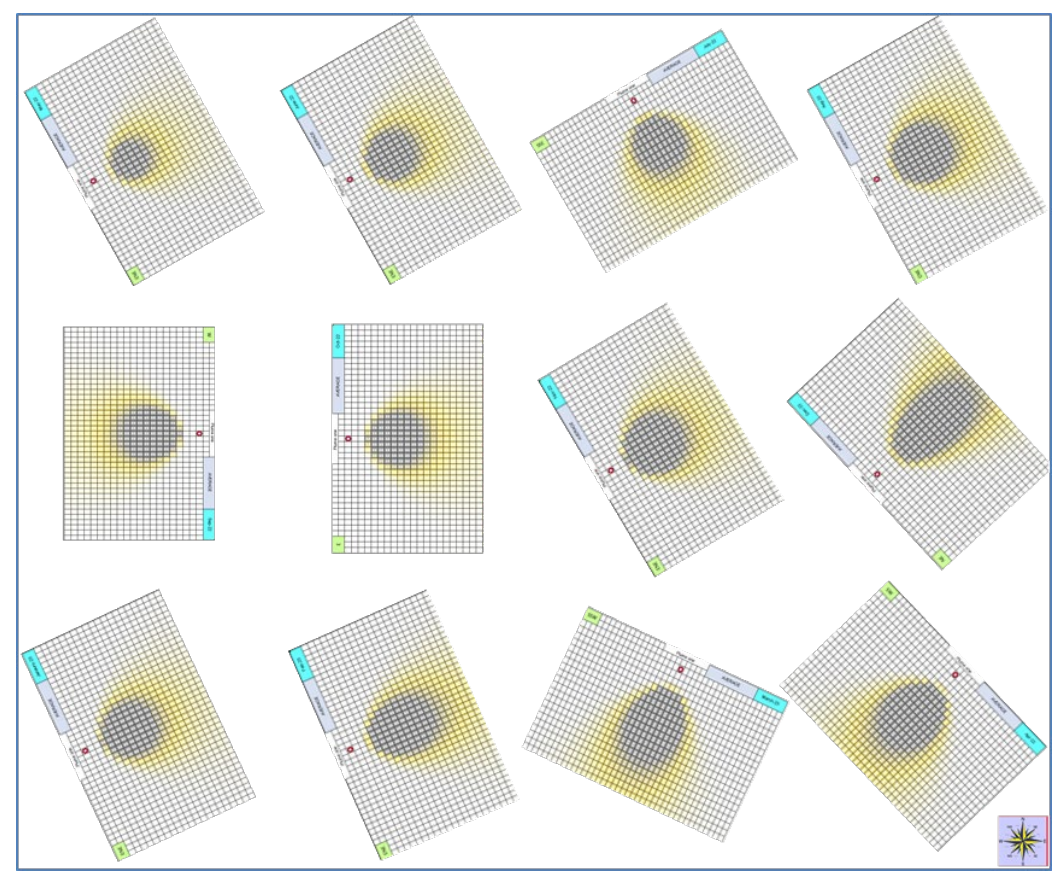


Fig. 9a. Condensed pollution points of Stack 1 for average daily CO₂ concentration

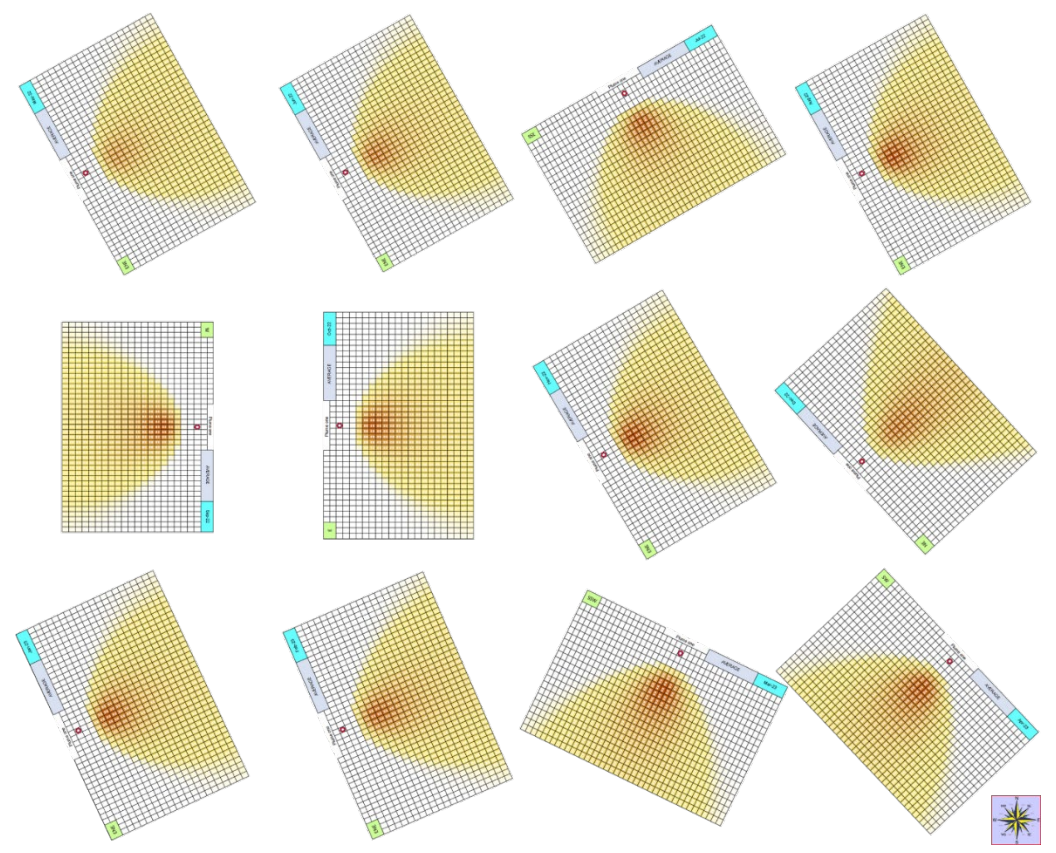


Fig. 9b. Condensed pollution points of Stack 1 for average daily SO₂ concentration

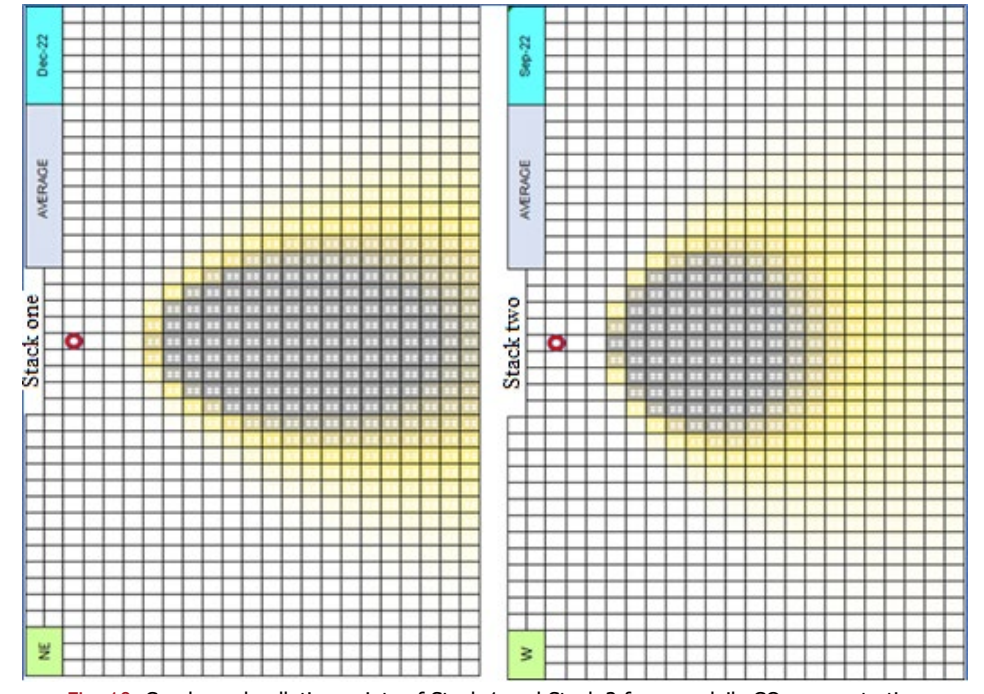


Fig. 10. Condensed pollution points of Stack 1 and Stack 2 for avg. daily CO₂ concentration

The CH_4 and N_2O emissions from Stack 1 and Stack 2 are almost very similar because the emission quantity and the effective stack height sensitivities on the concentrations are the same (Figures 11a and 11b).

The effective stack height sensitivities on the SO₂ concentrations are given in Figure 11c. As the stack height is decreasing, the ground level concentrations are increasing and the dispersion distance on both crosswind and horizontal axes are getting closer to the stack. The color of Stack 2 is denser than Stack 1.

Variation of Pollution Concentration on Maps: The pollution concentration maps are formed by using MATLAB software which is licensed to the Karabük University. The main aim of these figures is to show the dispersion of pollutants during transportation from month to month. The convections of emitted gases change considerably. The change is shown clearly in Figure 12.

The highest ground level concentration is reached in November 2022 as $4x10^{-4}$ g/m³. This quantity is two times more than the maximum value in May 2022, which is the lowest pollution month for this study. The highest emission is, moreover,

seen in July 2022. Therefore, the physical and atmospheric parameters are very important for the ground-level concentrations. When someone observes the general parameters for November 2022, it is seen that the atmospheric stability classes are "A", which is the most stable condition, and the average wind speed is just 1.65 m/s. It is a very low wind speed for the study. The atmospheric wind speed is very close to the natural convection and the dispersion cannot be enough to distribute the pollution over the atmosphere. The lowest ground-level concentrations were observed in May 2022. In May 2022, the highest concentration on the ground level is 2.3×10^{-4} g/m³.

The Stack 2 emissions create more ground-level concentrations than Stack 1 because the height of Stack 2 is half of Stack 1 with a value of 25 m. The highest CO₂ concentration is observed around 7.5x10⁻⁴ g/m³ in November 2022 and the lowest concentration is observed at 1.5x10⁻⁴ g/m³ again in May 2022. The highest concentration in May 2022 is only seen at one point with a value of 3x10⁻⁴ g/m³. For Stack 1 atmospheric emission is always higher, surprisingly Stack 1 concentrations on the ground level are also high.

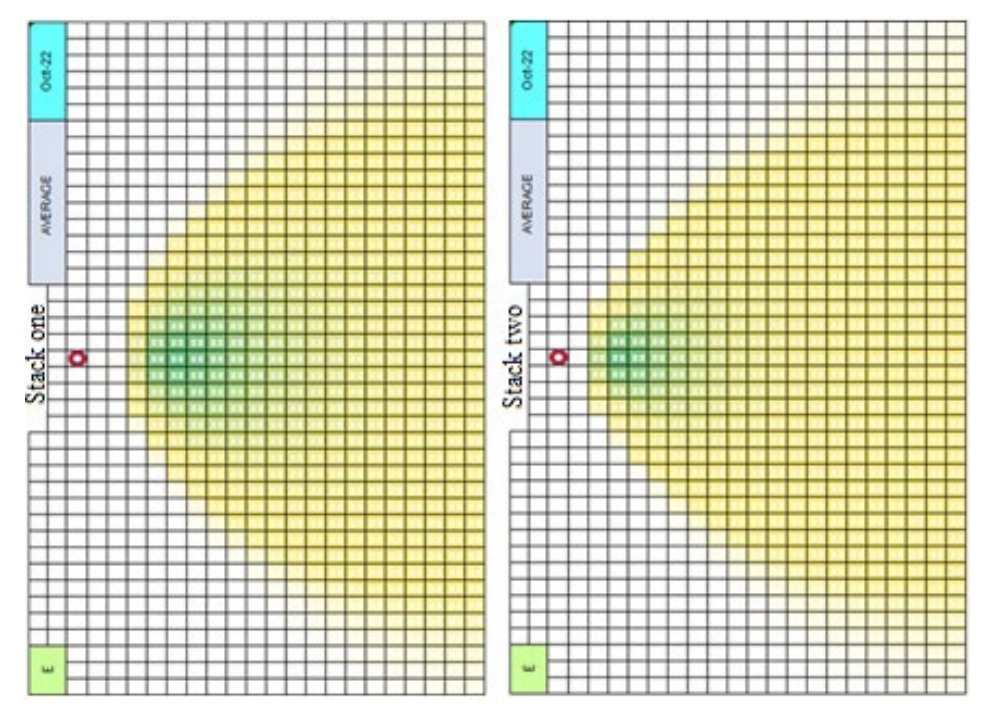


Fig. 11a. Pollution created by Stacks 1 and 2 for average daily CH₄ emissions in October 2022

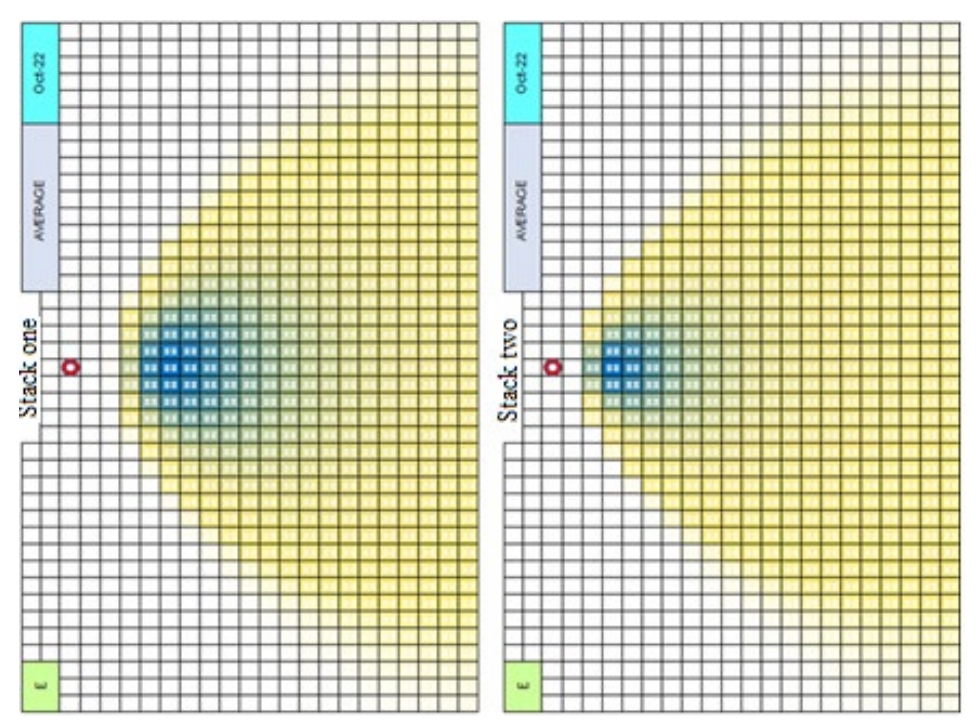


Fig. 11b. Pollution created by Stacks 1 and 2 for average daily N2O emissions in October 2022

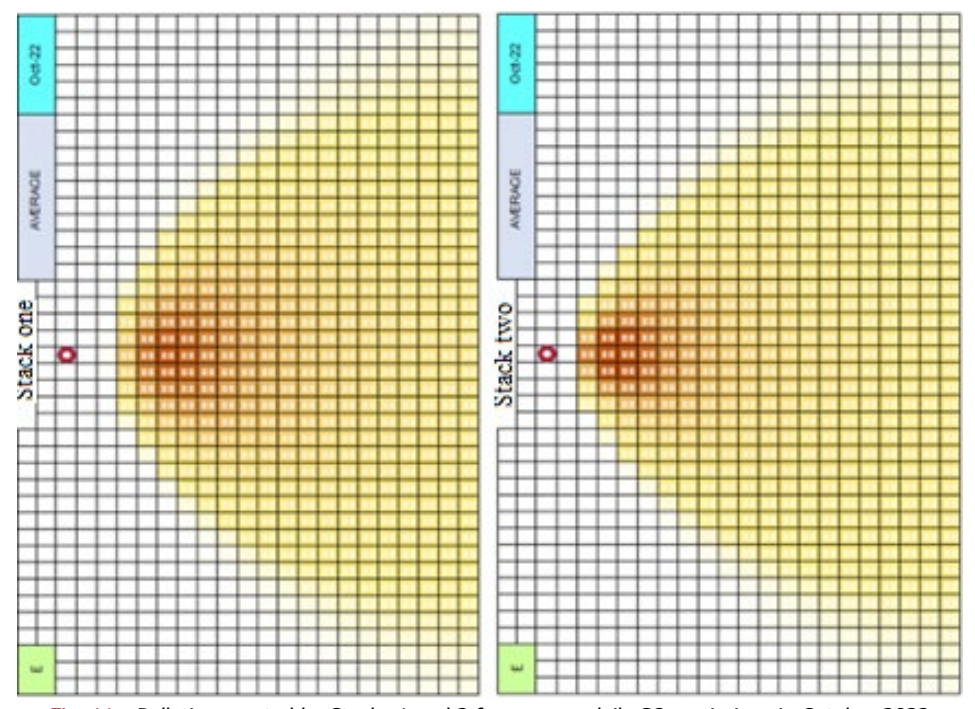
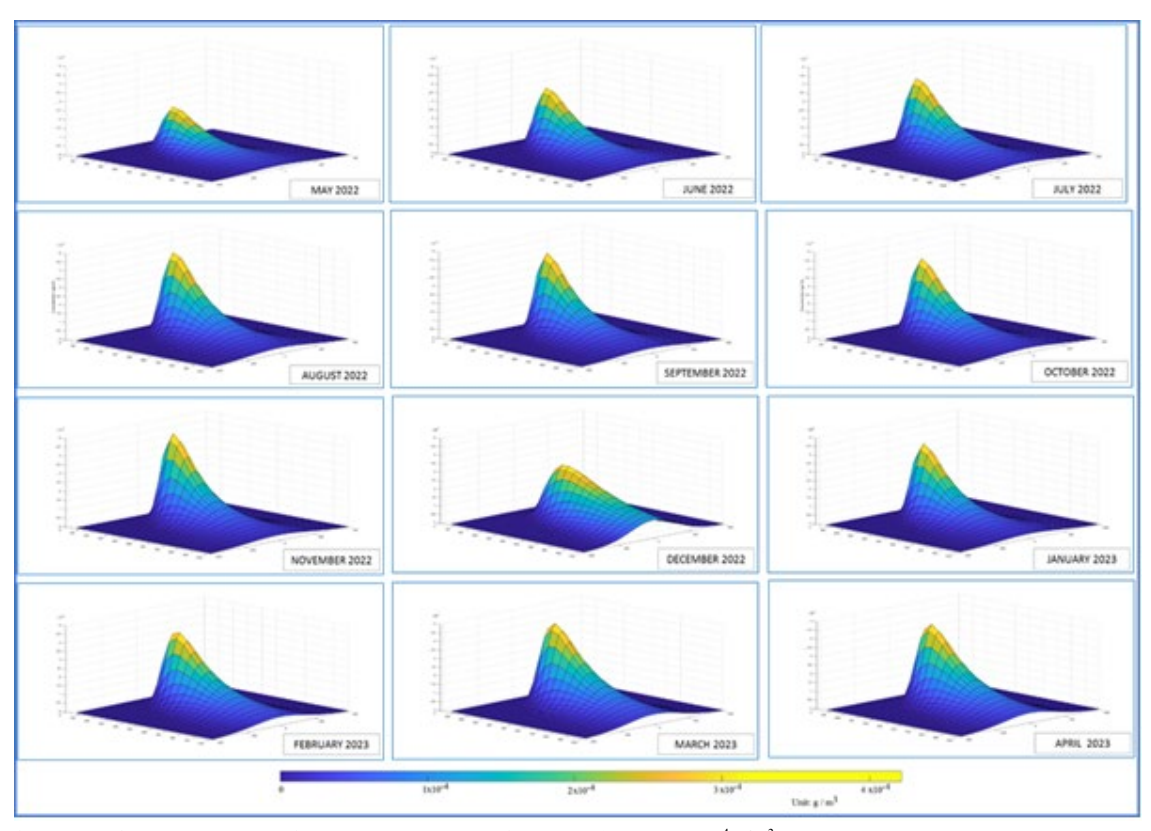


Fig. 11c. Pollution created by Stacks 1 and 2 for average daily SO₂ emissions in October 2022



*Note: X axis: 0 to 1000 m; Y axis: 500m to -500 m; Z axis (Concen.): 0 to 2.5x10⁻⁴ g/m³

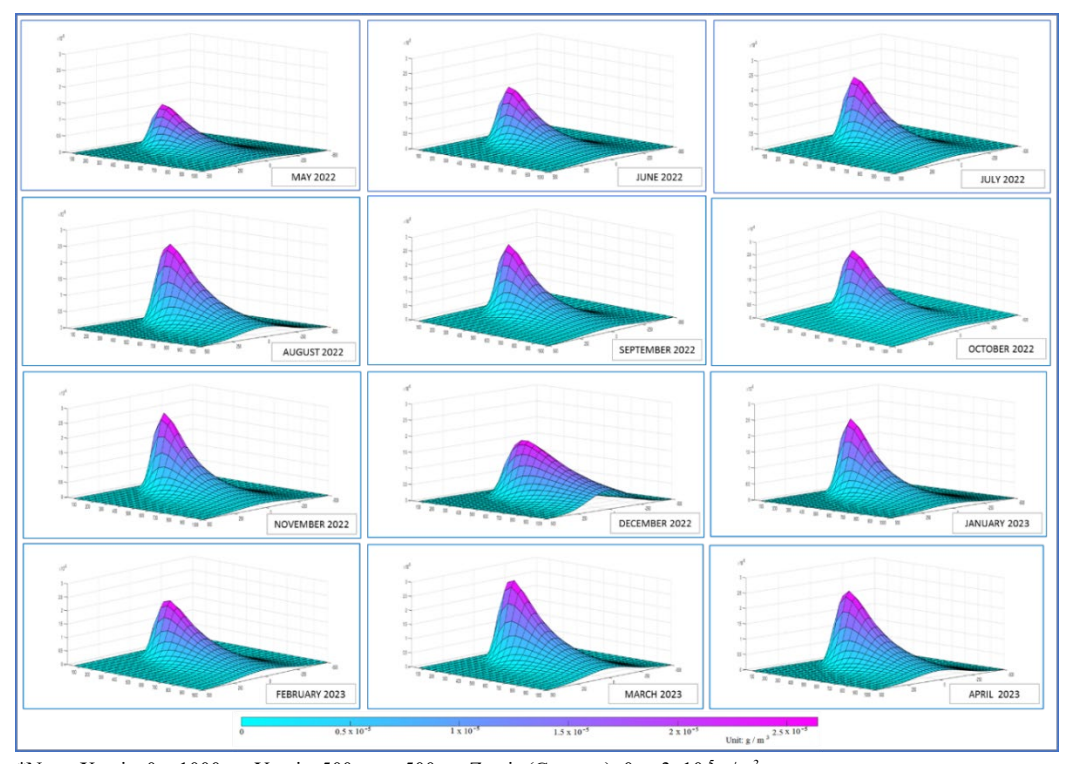
Fig. 12. Variation of pollution concentrations of Stack 1 for average daily CO₂

In other words, the atmospheric emission that is emitted to the atmosphere in the lowest elevation is expected to cause a higher ground level concentration. However, some other meteorological parameters, such as wind speed and stability classes can change the expected ground-level concentration.

The average CH₄ concentration graphs are evaluated seasonally. The concentration in June is lower than in the other months because of the wind speed. The average wind speed is around 2.16 m/s. With this wind speed transportation is seen to be high. High dispersion causes low ground-level concentrations. For Plume 1, the highest ground-level concentration is about 4.5x10⁻⁸ g/m³. The seasonal variation of N₂O concentration is lower. The highest ground-level concentrations are found to be 1.1x10⁻⁸ g/m³. This quantity may seem very low. However, the GWP (Global Warming Potential) of N₂O is much higher than the other GHGs.

The variation of ground-level concentrations for SO₂ gases is given in Figure 13. The ground level variation is parallel to the other pollutants. However, the SO₂ concentrations are more dangerous than the other gases due to severe effects on human health, flora, and buildings. The created ground-level concentrations only belong to the Stack 1 of the industry. This created quantity is after the application of desulphurization units. Even though the SO₂ emission control system is applied on the stacks, the emitted concentrations are still dangerous for the residents. The monthly ground level SO₂ concentrations are changing between 1.3 x 10⁻⁵ g/m³ in May 2022 and 2.6 x 10⁻⁵ g/m³ in November 2022.

The created ground-level concentrations for Stack 2 are given in Figure 14. The formed concentrations are still dangerous for the residents as the Stack 1.



*Note: X axis: 0 to1000 m; Y axis: 500m to -500 m; Z axis (Concen.): 0 to $3x10^{-5}$ g/m³ Fig. 13. Variation of pollution concentrations of Stack 1 for average daily SO_2

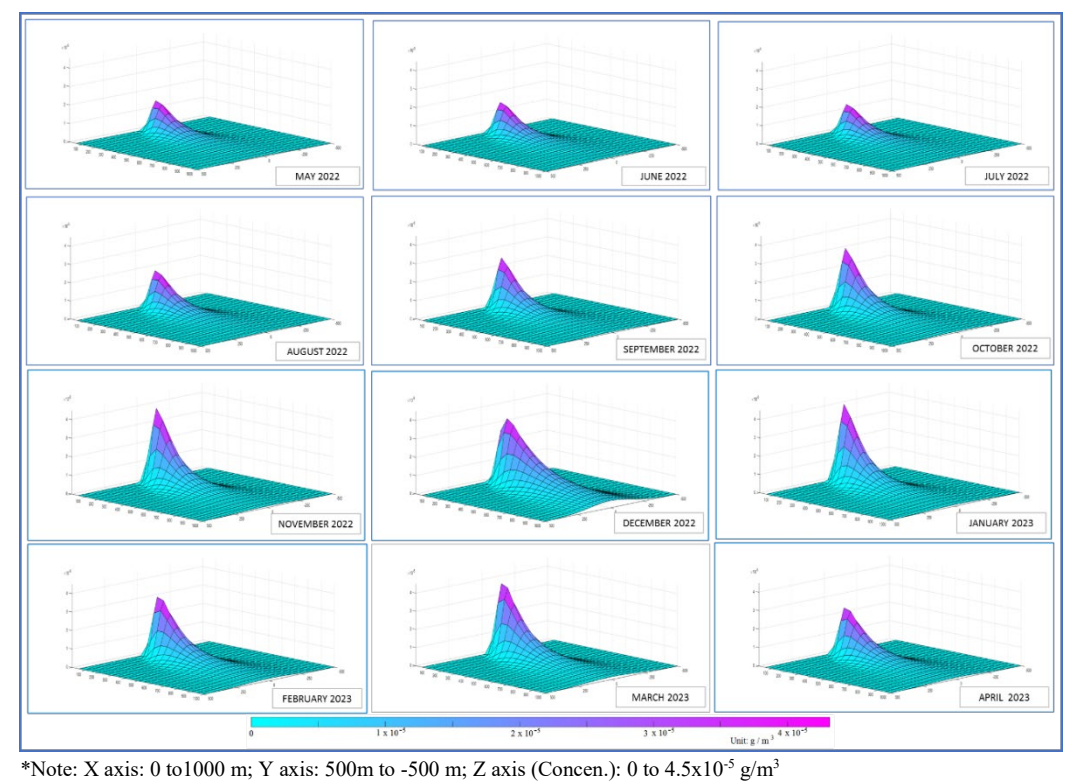


Fig. 14. Variation of pollution concentrations of Stack 2 for average daily SO₂

The monthly ground level SO₂ concentrations are changing between 1.6 x 10⁻⁵ g/m³ in July 2022 and 4.3 x 10⁻⁵ g/m³ in January 2023. It can be concluded that Stack 2 is dirtier than Stack 1, although it is claimed by the company that a 60% reduction in emissions is provided by the stack gas cleaning system.

As can be observed from Figure 14, the dispersion distance on both crosswind and horizontal axes is getting closer to Stack 2 than in the case of Stack 1. This means that residents located closer to the factory will be affected more by the emissions of SO₂. The main reason is the lowest stack height as it was described before.

4. Discussion

The mitigation activities dealing with controlling the emission rate is a progressive step for the climate change problems of the countries. Calculations are based on the IPCC Tier 1 approach. It is the simplest IPCC methodology. The main calculations depend on fuel consumption data and default emission factors. The conversion of units, combustion efficiency, carbon content and calories of fuels is very important for the exact calculations. Emissions of CO₂, CH₄ and N₂O, which are known as direct GHGs, are contributing to climate change considerably. For that reason, these emission data are selected for the dispersion. Emissions data of CO₂, CH₄, and N₂O are the most important parameters for the modeling.

The Gaussian Plume Model is implemented by using various software programs; however, this study focuses on using the Microsoft Excel Program. It is a powerful and practical tool for evaluating air pollution from point sources. The Excel base program was improved by Can [34] in 2023 to observe the emissions and dispersion of pollutants from industrial point sources over the area. The ground-level concentrations were studied. Some meteorological and physical parameters are very sensitive for the model. The results have shown that the dispersion does not only depend on atmospheric conditions but also depends on the physical conditions of industries. The stack height, effective plume height and pollutant emission

concentrations are very important variables for the industries. To use the GP Model for the industries, meteorological data needs to be collected from TSMS as described in the Methodology section. The atmospheric weather temperatures, cloudiness, wind speed and wind directions are the most sensitive parameters to determine atmospheric stability for the model.

The final step is to obtain the concentration maps by using GPM outputs. The outputs were obtained in two forms. The first one was the Excel Program output, which is the evaluation of Excel macros in the GPM Program. The second one is also an output of the GPM Program. The concentration data over the described zone is listed according to the x (wind direction), y (dispersion direction) and concentration. The listed data is used by MATLAB to evaluate concentrations in 3D form. The main goal is to see the affected areas according to the existing emissions from the plumes.

5. Conclusion

The development of the point source dispersion model, using MS Excel as the base, has been described in this study. The software application offers a user-friendly framework for estimating pollutant concentrations and assessing potential fatalities. By leveraging the capabilities of Microsoft Excel, the software streamlines the concentration estimation process, making it more efficient and accessible to users (Table A1 in Appendix A). The research of this study underlines the importance of employing software tools for air pollution assessment. The point source dispersion model represents a valuable contribution to the field, providing a practical and user-friendly approach to estimating pollutant concentrations. It also opens avenues for further advancements in air pollution modeling and highlights the potential of software applications in addressing challenges. Overall, the findings of this study contribute to enhancing our understanding of air pollution management and provide valuable insights for decision-makers and stakeholders involved in process industries.

This study can be applied to any industry which has a plume. For obtaining the general effect of the industries on the environment, this useful GPM Program can be used and a general idea about the emissions for any point source of industries can be obtained. In this study, the physical and atmospheric parameters are the main variables, and each parameter was tested to understand the sensitivity. The highest sensitivities are observed in the wind speed, stability class, plume height and emission from the plume. These parameters can ground-level concentrations change the unexpectedly. Atmospheric pollutants emitted to the atmosphere in the lowest elevation is expected to cause higher ground-level concentrations. However, some other meteorological parameters, such as wind speed and stability classes, can change the expected ground-level concentrations.

The main output of this study is to see the effects of the emission of a mid-size industrial establishment in Karabük Province. If the emission from the plumes of the industry is transported in the direction between northwest and northeast, the ground-level concentrations will affect the residential areas considerably. Public health even in

Declaration

Funding

This research received no external funding.

Author Contributions

A. Can: Conceptualization, Methodology, Software, Validation, Formal Analysis, Investigation, Writing, Reviewing, Editing, Visualization, Supervision. M. A. Lefghih: Writing - Original draft, Resources, Reviewing.

Acknowledgments

Not applicable.

low emissions could be in danger due to highly condensed ground-level concentrations. The sustainability of residential living standards in this area does not seem to be good. The local authorities can make some decisions and the residential area can be established away from this zone. The concentration level at low wind speed in the north direction, at a high rate of emission from the plume and atmospheric inversion conditions, affect people living in this zone adversely due to low ambient air quality. When the entire industrial establishments in the zone are considered, the present residential conditions will not be appropriate.

It will be very beneficial to apply the results and the output of this study to selecting new residential zones. Today's residential zone is almost full of many private one or two-floor houses. This zone is fully saturated. Urban transformation is a governmental plan to supply their citizens with an earthquake-resistant building. Therefore, the relocation of the city center to a less polluted area with highly resistant buildings to an earthquake will be the best solution for municipal residential planning.

Data Availability Statement

The data presented in this study are available on request from the corresponding author.

Ethics Committee Permission

Not applicable.

Conflict of Interests

The author(s) declared no potential conflicts of interest with respect to the research, authorship, and/or publication of this article.

References

[1] Fuller R, Landrigan PJ, Balakrishnan K, Bathan G, Bose-O'Reilly S, Brauer M, Caravanos J, Chiles T, Cohen A, Corra L, Cropper M, Ferraro G, Hanna J, Hanrahan D, Hu H, Hunter D, Janata G, Kupka R, Lanphear B, Lichtveld M, Martin K, Mustapha A,

- Sanchez-Triana E, Sandilya K, Schaefli L, Shaw J, Seddon J, Suk W, Téllez-Rojo MM, Yan C (2022) Pollution and health: a progress update. The Lancet Planetary Health 6(6): e535-e547.
- Glavovic BC, Smith TF, White I (2022) The [2] tragedy of climate change science. Climate and Devolopment 14(9):829-833.
- Seddon N, Smith A, Smith P, Key I, Chausson A, Girardin C, House J, Srivastava S, Turner B (2021) Getting the message right on nature-based solutions to climate change. Global Change Biology 27(8):1518-1546.
- [4] Almetwally AA, Bin-Jumah M, Allam AA (2020) Ambient air pollution and its influence on human health and welfare: an overview. Environmental Science and Pollutin Research 27: 24815-24830.
- Brancher M, Hoinaski L, Piringer M, Prata AA, Schauberger G (2021) Dispersion modelling of environmental odours using hourly-resolved emission scenarios: Implications for impact assessments. Atmospheric Environment 12:100124.
- Manisalidis I, Stavropoulou E, Stavropoulos A, Bezirtzoglou E (2020) Environmental and health impacts of air pollution: a review. Frontiers in Public Health 8: 14.
- Wang H, Rasch PJ, Easter RC, Singh B, Zhang R, Ma PL, Qian Y, Ghan SJ, Beagley N (2014) Using an explicit emission tagging method in global modeling of source-receptor relationships for black carbon in the Arctic: variations, sources, and transport pathways. Journal of Geophysical Research Atmospheres 119(12): 12888-12909.
- De Visscher A (2015) Air Dispersion Modeling: Foundations and Application. John Wiley & Sons, Hoboken.
- Vallero D (2014) Fundamentals of Air Pollution, Fifth Edition. Elsevier Academic Press.
- [10] Rusu-Zagar G, Rusu-Zagar C, Iorga I, Iorga A (2013) Air pollution particles PM10, PM2,5 and the tropospheric ozone effects on human health. Procedia-Social and Behavioral Science 92:826-
- [11] Morris SC (1984) Atmospheric pollution, its history, origins and prevention: (1981) 4th edition, By A. R. Meetham. Pergamon Press, Oxford. Environment International 10(3): 270–271.
- [12] Fowler D, Brimblecombe P, Burrows J, Heal MR, Grennfelt P, Stevenson DS, Jowett A, Nemitz E, Coyle M, Lui X, Chang Y, Fuller GW, Sutton MA, Klimont Z, Unsworth MH, Vieno M (2020) A

- chronology of global air quality. Philosophical Transactions of the Royal Society A 378(2183): 20190314.
- [13] International Energy Agency (IEA) (2020) Statistics Report: CO2 Emissions from Fuel Combustion. CO2 Emiss. from fuel Combust. dataset. 13.
- [14] Johnson JB (2022) An introduction to atmospheric pollutant dispersion modelling. Environmental Sciences Proceedings 19(1): 18-20.
- [15] Holmes NS, Morawska L (2006) A review of dispersion modelling and its application to the dispersion of particles: an overview of different models available. Atmospheric dispersion Environment 40(30): 5902-5928.
- [16] Turner DB (2020) Workbook of Atmospheric Dispersion Estimates: An Introduction Dispersion Modeling, Second Edition. CRC Press.
- [17] Liu C, Zhou R, Su T, Jiang J (2022) Gas diffusion model based on an improved Gaussian plume model for inverse calculations of the source strength. Journal of Loss Prevention in the Process Industries 75:104677.
- [18] Assegaf AH (2018) Gas dispersion modeling from the chimney power plant pasquil-Gaussian Model. Journal of Natural Resources and Environmental Management 8(3): 414-419.
- [19] El-Harbawi M (2013) Air quality modelling, simulation, and computational methods: a review. Environmental Reviews 21(3): 149-179.
- [20] Ivaskova M, Kotes P, Brodnan M (2015) Air pollution as an important factor in construction materials deterioration in Slovak Republic. Procedia Engineering 108: 131-138.
- [21] Yoshino A, Takami A, Hara K, Nishita-Hara C, Hayashi M, Kaneyasu N (2021) Contribution of local and transboundary air pollution to the urban air quality of Fukuoka, Japan. Atmosphere 12(4): 431.
- [22] Almetwally AA, Bin-Jumah M, Allam AA (2020) Ambient air pollution and its influence on human health and welfare: an overview. Environmental Science and Pollution Research 27: 24815-24830.
- [23] Büke T, Köne AÇ (2016) Assessing air quality in Turkey: a proposed, air quality index. Sustainability 8(1):73.
- [24] Elbir T, Müezzinoğlu A, Bayram A (2000) Evaluation of some air pollution indicators in Turkey. Environment International 26(1-2): 5-10.

- [25] Özden Ö, Döğeroğlu T, Kara S (2008) Assessment of ambient air quality in Eskişehir, Turkey. Environment International 34(5): 678-687.
- [26] Baklanov A, Zhang Y (2020) Advances in air quality modeling and forecasting. Global Transitions 2: 261-270.
- [27] Badach J, Voordeckers D, Nyka L, Van Acker M (2020) A framework for air quality management zones - useful GIS-based tool for urban planning: case studies in Antwerp and Gdańsk. Building and Environment 174: 106743.
- [28] Cassiani M, Stohl A, Eckhardt S (2013) The dispersion characteristics of air pollution from the world's megacities. Atmospheric Chemistry and Physics 13(19): 9975-9996.
- [29] Gommes D, Watterson J (2006) Chapter 2: Stationary Combustion, 2.1 Volume 2: Energy. In: 2006 IPCC Guidelines for National Greenhouse Gas Inventories.
- [30] Shamsuddin SD, Omar N, Koh MH (2017) Development of radionuclide dispersion modeling software based on Gaussian Plume model. MATEMATIKA: Malaysian Journal of Industrial and Applied Mathematics 149-157.
- [31] Seibert P, Beyrich F, Gryning SE, Joffre S, Rasmussen A, Tercier P (2000) Review and intercomparison of operational methods for the determination of the mixing height. Atmospheric Environment 34(7):1001-1027.
- [32] Pasquill F (1976) Atmospheric dispersion parameters in Gaussian plume modeling: Part II. Possible Requirements for Change in the Turner Workbook Values.
- [33] Awasthi S, Khare M, Gargava P (2006) General plume dispersion model (GPDM) for point source emission. Environmental Modeling & Assessment 11: 267-276.
- [34] Can A (2023) 2D Gaussian Plume Model Excell Base Macro Programme.
- [35] IPCC (2001) Climate Change 2001: The Scientific Basis. Contribution Working Group I to the Third Assessment Report of the Intergovernmental Panel on Climate Change. Cambridge University Press.
- [36] Beychok MR (2005) Fundamentals of Stack Gas Dispersion, Fourth Edition.
- [37] Riddle A, Carruthers D, Sharpe A, McHugh C, Stocker J (2004) Comparisons between FLUENT and ADMS for atmospheric dispersion modelling. Atmospheric Environment 38(7): 1029-1038.
- [38] Perry SG, Cimorelli AJ, Paine RJ, Brode RW, Weil JC, Venkatram A, Wilson RB, Lee RF, Peters WD

- (2005) AERMOD: A Dispersion model for industrial source applications. Part II: Model performance against 17 field study databases. Journal of Applied Meteorology 44(5): 694-708.
- [39] Stohl A, Forster C, Frank A, Seibert P, Wotawa G (2005) The Lagrangian particle dispersion model FLEXPART version 6.2. Atmospheric Chemistry and Physics 5(9): 2461-2474.
- [40] Cora MG, Hung YT, Pagan-Rodriguez D (2003) Air dispersion modeling: using SCREEN3 to determine the MAGLC of air toxics. Environmental Quality Management 12(4): 67-67.
- [41] Binkowski FS, Roselle SJ (2003) Models-3 community multiscale air quality (CMAQ) model aerosol component 1. model description. Journal of Geophysical Research: Atmospheres 108(D6).
- [42] Fthenakis VM (1999) HGSYSTEM: a review, critique, and comparison with other models. Journal of Loss Prevention in the Process Industries 12(6): 525-531.
- [43] Guttikunda SK, Jawahar P (2018) Evaluation of particulate pollution and health impacts from planned expansion of coal-fired thermal power plants in India using WRF-CAMx modeling system. Aerosol and Air Quality Research 18(12): 3187-3202.
- [44] Claggett M (2014) Comparing predictions from the CAL3QHCR and AERMOD models for highway applications. Transportation Research Record 2428(1): 18-26.
- [45] Sykes I (2010) Scipuff capabilities and application in hazard assessment. In: HARMO 2010-Proceedings of the 13th International Conference on Harmonisation within Atmospheric Dispersion Modelling for Regulatory Purposes 450–454.

Appendix A

Table A1. Model comparison: features and performance

| Reference | Model name | Model type | Pollutant type | Advantages | Disadvantages |
|-----------|---|---|---|--|---|
| [36] | SLAB | Steady-state plume and transient puff models | Toxic chemicals | Agrees well with available field data. | Does not calculate source emission rates. |
| [37] | Atmospheric dispersion modelling system (ADMS) | Advanced Gaussian model | Primary pollutants continuous releases of toxic and hazardous waste products | Treats a wide variety of source conditions. | Run time can be long. |
| [38] | AERMOD | Steady-state Gaussian plume model | Primary pollutants | Flexibility in structuring the input files. | Dispersion of heavier-than-air gases is not considered. |
| [39] | FLEXPART | Lagrangian Particle Dispersion Model | SO ₂ , CO, Pb, PM _{2.5} . PM ₁₀ | Requires a short computation time. | Cannot diagnose surface fluxes of moisture. |
| [40] | SCREEN3 | Gaussian plume model | SO ₂ , H ₂ S, CO, NH ₃ , VOCs, PM _{2.5} , PM ₁₀ , Fugitive emissions and/or deposition | Has some accounting for building effects. | Only predicts concentrations. |
| [41] | Community multiscale air quality (CMAQ) | Eulerian grid model | Multipollutant (ozone, fine particles, VOC, toxics, acid deposition, and visibility degradation) | Can be used for urban and regional scale. | Supports just one- way grid nesting. |
| [42] | Dispersion models for ideal gases and hydrogen fluoride | Four types of dispersion models: HFPLUME, PLUME, PGPLUME, and HEGADAS | Two-phase multicompound mixture of nonreactive chemicals or hydrogen fluoride with chemical reactions | One of the best available atmospheric dispersion models. | It is not as user- friendly. |
| [43] | Comprehensiv e air quality model with extensions (CAMx) | Multiscale, 3D Eulerian photochemical grid model | O ₃ formation from NO _x and volatile organic compound emissions; PM _{2.5} , PM ₁₀ , and PM components; CO | Computationally efficient and easy to use. | Spatial resolution is limited. |
| [44] | CAL3QHCR | Steady-state Gaussian model | CO, PM , and Inert pollutants | Able to model a variety of roadway characteristics situations. | Not valid for analysis of link heights >30 ft. |

| Table A1. Cor | nt'd | | | | |
|---------------|-------------------|------------------------|--------------------|--|--|
| [45] | SCIPUFF | Gaussian puff model | Primary pollutants | Performs accurate treatment of wind shear. | Not widely available and not extensively documented. |
| [34]* | INDUSTRIAL GPM | Gaussian puff model | Primary pollutants | Perform in short time, accurately and point specific. The condense polluted area is easy to be determined. | The output is transferred for detail concentration analyses. |

^{*} The used model in this study

Appendix B

Table B1. Emission Factors for GHGs

| | CO ₂ Facto | ors | | CH ₄ Fa | ctors | N ₂ O Factors | |
|------------|--------------------------------------|------------|-------------------|--------------------|---------------------------|--------------------------|---------------------------|
| Fuel Types | CO ₂ EF Unit: tC/TJ | Efficiency | C-CO ₂ | Fuel Types | Industry EF (Kg/TJ) | Fuel Types | Industry EF (Kg/TJ) |
| Lignite | 27.6 | 0.980 | 3.6667 | Lignite | 10 | Lignite | 1.4 |
| Fuel-Oil | 21.1 | 0.990 | 3.6667 | Fuel-Oil | 2.0 | Fuel-Oil | 0.6 |

Table B2. Emission Factors for SO₂

| SO ₂ f | actors |
|-------------------|---------------------|
| Fuel Types | Industry EF (Kg/TJ) |
| Lignite | 5700 |
| Fuel Oil | 5714 |

Table B3. Variables for SO₂

| EFso ₂ (kg/TJ) | s (%) | r (%) | n (efficiency) | Q (TJ/kt) |
|---------------------------|-------|-------|----------------|-----------|
| 5700 | 1.5 | 5 | 60 | 20 |
| 5714 | 3 | 0 | 60 | 42 |



$$EF_{SO_2} = 2 \times \left(\frac{s}{100}\right) \times \left(\frac{1}{Q}\right) \times 10^6 \times \left(\frac{100 - r}{100}\right) \times \left(\frac{100 - n}{100}\right)$$

where

EF_{SO2} : SO₂ emission factor (kg/TJ)

2 : SO₂/S ratio (kg/kg)

s : Sulphur content in fuel (%)
 r : Retention of Sulphur in ash (%)
 Q : Net calorific value (TJ/kt)

10 6 : Unit conversion factor

n : Efficiency of abatement technology and/or reduction efficiency (%)

Appendix C

Table C1. Examples of GPM Program inputs for Stack 1 and Stack 2

| Table C1. Examples of GPM Program inp | | | | |
|---|--|-----------------------|--|--|
| Description (1st Stack) | Unit | Symbol | Value | |
| Concentration | g/m³ | Х | | |
| Emission rate | g/s | Q | 0,7827641 | |
| Wind Speed | m/s | u | 1,65 | |
| Physical Stack Height | m | h | - | |
| Effective Stack Height | m | Н | 53 | |
| Wind Direction | | | ENE | |
| Stability Class Code | | | 1 | |
| MAX X DISTANCE (km) (100 m - 20000 | m) | | 1000 | |
| MAX Y DISTANCE (km) (0.0 m - 5000 n | n) | | 500 | |
| WHICH Z HEIGHT (km) (min: 0.0 m - 20 | 000 m) | | 0 | |
| WHICH MONTH? | | | Kas.22 | |
| SELECT(AVERAGE), (MAXIMUM), (MIN | IIMUM) | | AVERAGE | |
| X GRID LENGHT (km) | | | 50 | |
| Y GRID LENGHT (km) | | | 25 | |
| | | | | |
| D ' (2 15(1) | TT ' | G 1 1 | 77.1 | |
| Description (2nd Stack) | Unit | Symbol | Value | |
| Concentration | g/m ³ | X | | |
| Concentration Emission rate | g/m³ g/s | | 0,4057009 | |
| Concentration Emission rate Wind Speed | g/m ³ | X Q u | | |
| Concentration Emission rate Wind Speed Physical Stack Height | g/m³ g/s | X Q u h | 0,4057009 | |
| Concentration Emission rate Wind Speed Physical Stack Height Effective Stack Height | g/m³ g/s m/s | X Q u | 0,4057009 | |
| Concentration Emission rate Wind Speed Physical Stack Height | g/m³ g/s m/s m | X Q u h | 0,4057009 1,65 | |
| Concentration Emission rate Wind Speed Physical Stack Height Effective Stack Height | g/m³ g/s m/s m | X Q u h | 0,4057009 1,65 - 28 | |
| Concentration Emission rate Wind Speed Physical Stack Height Effective Stack Height Wind Direction | g/m³ g/s m/s m | X Q u h | 0,4057009 1,65 - 28 ENE | |
| Concentration Emission rate Wind Speed Physical Stack Height Effective Stack Height Wind Direction Stability Class Code | g/m ³ g/s m/s m m | X Q u h | 0,4057009 1,65 - 28 ENE 1 | |
| Concentration Emission rate Wind Speed Physical Stack Height Effective Stack Height Wind Direction Stability Class Code MAX X DISTANCE (km) (100 m - 20 | g/m ³ g/s m/s m m 00000 m) | X Q u h | 0,4057009 1,65 - 28 ENE 1 1000 | |
| Concentration Emission rate Wind Speed Physical Stack Height Effective Stack Height Wind Direction Stability Class Code MAX X DISTANCE (km) (100 m - 20 MAX Y DISTANCE (km) (0.0 m - 50 | g/m ³ g/s m/s m m 00000 m) | X Q u h | 0,4057009 1,65 - 28 ENE 1 1000 500 | |
| Concentration Emission rate Wind Speed Physical Stack Height Effective Stack Height Wind Direction Stability Class Code MAX X DISTANCE (km) (100 m - 20 MAX Y DISTANCE (km) (0.0 m - 50 WHICH Z HEIGHT (km) (min: 0.0 m | g/m ³ g/s m/s m m | X Q u h H | 0,4057009 1,65 - 28 ENE 1 1000 500 | |
| Concentration Emission rate Wind Speed Physical Stack Height Effective Stack Height Wind Direction Stability Class Code MAX X DISTANCE (km) (100 m - 20 MAX Y DISTANCE (km) (0.0 m - 50 WHICH Z HEIGHT (km) (min: 0.0 m) WHICH MONTH? | g/m ³ g/s m/s m m | X Q u h H | 0,4057009 1,65 - 28 ENE 1 1000 500 0 Kas.22 | |